euronoise

Effects of internal waves on acoustic coherent communications during SW06

Aijun Song[a], Mohsen Badiey[a], Arthur Newhall[b], James Lynch[b] and Harry Deferrari[c]

[a]University of Delaware, College of Marine and Earth Studies, S. College Street, Newark, DE 19716, USA
[b]Woods Hole Oceanographic Institution, 98 Water Street, Bigelow 203A, MS-11, Woods Hole, MA 02543, USA
[c]Univ. of Miami, 4600 Rickenbacker Causeway, Miami, FL 33149, USA
ajsong@udel.edu

During a 12 h period in the Shallow Water 2006 experiment, concurrent environmental observations and acoustic measurements were made to study internal wave effects on coherent underwater acoustic communications. Binary phase shift keying signals at carrier frequencies 813 Hz and 1627 Hz which propagated over a 19.8 km source-receiver range during the 12 h period are processed. This is done using time reversal multichannel combining followed by a decision feedback equalizer with continuous channel updates prior to time reversal combining. The communications performance in terms of output signal-to-noise ratio exhibits significant change (more than 5 dB) due to the passage of internal waves through the acoustic track. The effects of the internal waves also show a frequency dependency.

1 Introduction

It is well known that internal waves can cause significant fluctuations of acoustic pulses propagating in shallow water [1]. There have been a number of experimental and modeling efforts to investigate the internal wave effects on acoustic wave propagation in shallow water. For example, intensity fluctuations of acoustic pulses caused by internal waves were reported and modeled based on the SWARM'95 experiment [2, 3]. The coherence properties of acoustic pulses in an internal wave field have also been studied [4]. Both coherence and intensity fluctuation properties of the acoustic channel can affect the performance of coherent underwater acoustic communications. Therefore, it is expected that internal waves can have a dramatic impact on receiver performance. However, only limited efforts have been made and reported to quantify these effects. One notable example of such work is that of T. C. Yang [5], where the channel temporal coherence in the presence of internal waves was reported and related to the equalizer behavior.

During the Shallow Water 2006 (SW06) experiment [6], concurrent environmental observations and acoustic measurements were made to study the internal wave effects on coherent underwater acoustic communications. During a 12 h period, a packet of strong internal waves was observed to pass through a 19.8 km acoustic track over which binary phase shift keying (BPSK) signals were transmitted every 30 min. In this paper, the BPSK signals at the carrier frequencies of 813 Hz and 1627 Hz are demodulated by a recently developed multichannel receiver [7]. The receiver employs time reversal multichannel combining followed by a single channel decision feedback equalizer (DFE). Continuous channel updates are performed prior to time reversal combining to track channel fluctuations during a data packet. The performance of the communication receiver in terms of output signal-to-noise ratio (SNR) is reported over the entire period when the internal waves passed through the acoustic track. The objective of this study is to show the extent of the internal wave effects on coherent underwater acoustic communications. It is also intended to show the frequency dependency of the internal wave effects exhibited at the carrier frequencies of 813 Hz and 1627 Hz. Note all time information in the paper is in Greenwich Mean Time (GMT).

2 Experimental settings

The SW06 experiment was conducted east off the New Jersey continental shelf from July to September of 2006 [6]. During the experiment, the University of Delaware (UDEL) science team on the R/V Sharp studied the azimuthal effects of internal waves on acoustic wave propagation. The experimental activities performed by the UDEL team were named after the internal wave events observed by the R/V Sharp. For example, in this paper, the period from 18:00 on Aug. 17 to 06:00 on Aug. 18, 2006 is referred to as Event 50, as will be discussed. The acoustic source used was denoted as the Miami Sound Machine (MSM) and was deployed about 19.8 km from the 16 element Woods Hole Oceanographic Institution vertical line array (WHOI-VLA). The water depth was about 80 m along the entire acoustic track. The WHOI-VLA spanned approximately the entire water column. The experimental setting is shown in Fig. 1. During Event 50, two research vessels, the R/V Sharp and the R/V Oceanus, coordinated operations to monitor the formation and propagation of internal waves using their onboard radars. At 18:00 on Aug. 17, 2006, the two research vessels kept stationary southeast of the WHOI-VLA, the R/V Sharp at location A_1 and the R/V Oceanus at location B_1 in Fig. 1, observing the formation of a packet of strong internal waves. As the packet propagated northwest, the two research vessels then followed the internal wave front. At around 21:30, the observed internal wave packet started to intersect the acoustic track. The observed internal wave packet is shown in Fig. 1 at 22:30 when the R/V Sharp was at location A_2 and the R/V Oceanus was at location B_2. As shown, the internal wave packet had a large overlap with the acoustic track at 22:30. At around 02:00 on Aug. 18, the internal wave packet started to move off the acoustic track. The internal wave observation also can be confirmed by the temperature profiles recorded at the sensors attached to the WHOI-VLA mooring [6] as shown in Fig. 4(a).

Two different BPSK signals, transmitted from the MSM in succession every 30 min during Event 50, will be analyzed here: 1) the 90 s BPSK signal at a carrier frequency of $f_c = 813$ Hz and 2) the 80 s BPSK signal at $f_c = 1627$ Hz. The symbol rate R of the signals is one fourth of the carrier frequency f_c, i.e., $R = f_c/4$. The source level at the two carrier frequencies was 186 dB re 1 μPa at 1 m.

3 Receiver structure

Consider an underwater acoustic transmitter and receiver deployed in shallow water. At the source, a binary information sequence $x(n)$ is transformed into a baseband continuous wave $x(t)$. Then $x(t)$ is modulated onto the carrier frequency f_c and transmitted from a sound transducer. Let the total number of the hydrophones at the receiver be M and $y^{(i)}(t)$ be the received baseband signal at the i^{th} hydrophone. The effect of the transmis-

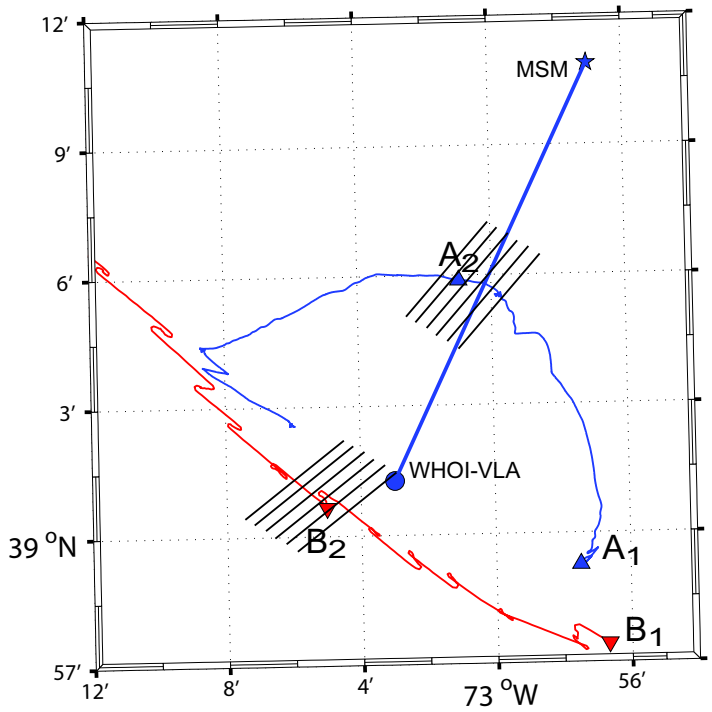

Figure 1: The experimental setting from 18:00 on Aug. 17 to 06:00 on Aug. 18, 2006 (Event 50). The MSM was the acoustic source and the WHOI-VLA was the receiver. The source-receiver range is about 19.8 km. The water depth is about 80 m along the acoustic track. The ship tracks of the R/V Sharp and R/V Oceanus are $A_1 - A_2$, $B_1 - B_2$, respectively. The parallel lines around A_2 and B_2 illustrate the observed internal waves at 22:30 on Aug. 17, 2006. The observed internal waves by the two vessels are known to be the two segments of the same internal wave packet.

sion medium between the source and the i^{th} hydrophone can be characterized by a time-varying channel impulse response (CIR) function, $h^{(i)}(t,\tau)$. Therefore, we can write

$$y^{(i)}(t) = x(t) \circledast h^{(i)}(t,\tau) + v^{(i)}_{amb}(t), \qquad (1)$$

where $v^{(i)}_{amb}(t)$ represents the ambient noise and $\circledast$ denotes the convolution operation.

To recover the transmitted symbols which have been passed through the fluctuating multi-path acoustic waveguide, time reversal multichannel combining followed by DFE is used. Channel estimation is performed frequently to track channel fluctuations. Here, frequently means multiple times over scales of seconds. Compensation for residual phase fluctuations and intersymbol interference after time reversal combining is done using a DFE [7]. The receiver structure is shown in Fig. 2.

Although time reversal based, the employed receiver [7] has a different structure than the time reversal DFEs [8,9] where multichannel combining is performed based on channel probes or the known symbols at the beginning of the data packet. The employed receiver [7] performs frequent channel estimation to track channel fluctuations which occur over scales of few seconds. Generally, faster fluctuating channels requires more frequent channel estimation.

The receiver is a channel estimation based structure. At the beginning of a data packet, a preamble, or a sequence of known symbols, is used to perform initial channel estimation and to adaptively train the DFE tap weights. After the preamble, the channel estimates are updated at an interval T_U. The most recent channel estimate on the i^{th} channel is denoted by $\hat{h}^{(i)}(t,\tau)$. The channel estimate $\hat{h}^{(i)}(t,\tau)$ can be obtained from the received signal and the previously detected symbols $\hat{x}(n)$ or the known symbols $x(n)$ during the preamble. The iterative least squares QR (LSQR) algorithm is used for channel estimation [10]. The channel estimation duration T_E is chosen to be twice the considered channel length T, i.e., $T_E = 2T$.

Time reversal multichannel combining uses $(\hat{h}^{(i)}(t,-\tau))^*$ to matched-filter the signals on each channel $y^{(i)}(t)$ and then combines the results [8, 9]. The output of time reversal combining is

$$r(t) = \sum_{i=1}^{M} (\hat{h}^{(i)}(t,-\tau))^* \circledast y^{(i)}(t) = x(t) \circledast q(t,\tau) + w(t), \qquad (2)$$

where * denotes the complex conjugate, $w(t)$ is the noise component, and $q(t,\tau)$ is the effective CIR function as

$$q(t,\tau) = \sum_{i=1}^{M} (\hat{h}^{(i)}(t,-\tau))^* \circledast h^{(i)}(t,\tau). \qquad (3)$$

A single channel DFE with joint phase tracking [11] is used to equalize the residual intersymbol interference in $r(t)$ of Eq. (2). An exponentially weighted recursive least-squares (RLS) algorithm is used to update the equalizer tap weights. The residual carrier phase offset in $r(n)$ is compensated for by a second order phase locked loop (PLL) embedded in the adaptive channel equalizer.

To measure the communication performance, the SNR at the soft output, $\tilde{x}(n)$ in Fig. 2, of the DFE is used. In the next section, the output SNR of the communica-

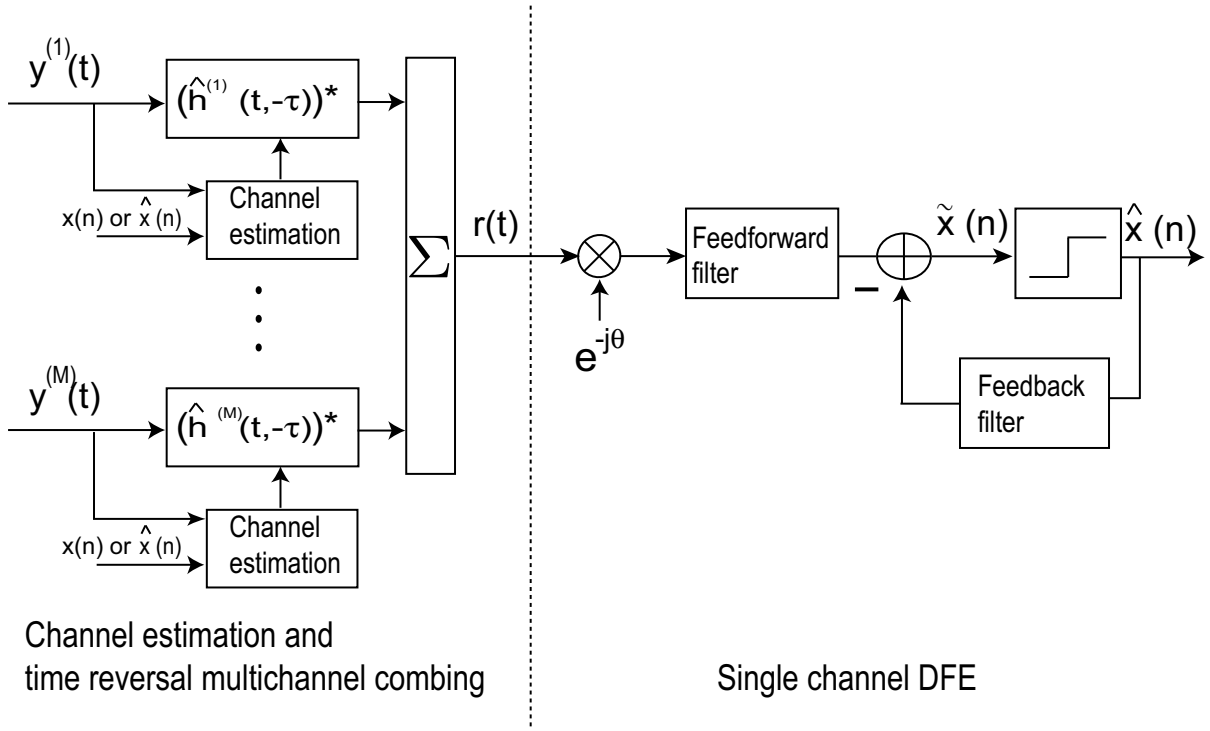

Figure 2: The employed receiver consists of time reversal multichannel combining followed by a DFE. Frequent channel estimation is performed to track channel fluctuations. A second order PLL embedded in the DFE is used to track the residual carrier phase offset after time reversal combining.

tion receiver is shown for the selected 12 h period in the SW06 experiment.

4 Communication performance results

Due to the presence of internal waves, the CIR function shows variable characteristics during Event 50. Figure 3 shows the CIR function at 77.25 m below the sea surface on the WHOI-VLA at two carrier frequencies at two geotimes. The CIR functions are obtained by the channel estimator in the receiver. As shown in Fig. 3(a), the CIR function at the carrier frequency of $f_c = 813$ Hz exhibits a slow variation during 90 s at 18:00, before the internal waves reached the acoustic track. In contrast, as shown in Fig. 3(b), the CIR function fluctuates at a faster rate in terms of coherence and intensity at 22:30 when the internal waves were intersecting the acoustic track. At $f_c = 1627$ Hz, the CIR function also shows a sharp contrast between 18:00 and 22:30.

As a consequence of the different channel characteristics, the receiver performance shows clear distinction between the two geotimes. Using the same set of receiver parameters, the receiver output SNR at 18:00 is 17.4 dB while it is 12.4 dB at 22:30 for the BPSK signal at $f_c = 813$ Hz. For the BPSK signal at $f_c = 1627$ Hz, the difference is smaller (1.8 dB) with the output SNR 15.9 dB at 18:00 versus 14.1 dB at 22:30. The reason might be due to the fact acoustic signals at higher frequencies can be affected by small scale fast environmental processes other than internal waves.

In the communication receiver, only 14 elements of the WHOI-VLA that covered the water column from depth 13.5 m to 77.25 m are used. The received data are oversampled with an oversampling rate $K = 4$. At the beginning of the BPSK packet, a 5 s preamble is used to carry out initial channel estimation and DFE tap weight training. The channel update interval is $T_U = 250$ ms. Such channel update rate is determined by searching over a range of values from $T_U = 125$ ms to $T_U = 2$ s. Decreasing $T_U = 250$ ms further only brings minimum performance improvement even at $f_c = 1627$ Hz in the presence of internal waves. The estimated CIR duration is $T = 330$ ms for the BPSK signal at $f_c = 813$ Hz and $T = 250$ ms at $f_c = 1627$ Hz. The channel estimation duration is $T_E = 2T$. The number of the feedforward taps is $KN_{ff} = 40$ for the fractionally spaced DFE [11] where $N_{ff} = 10$ is the feedforward filter span in symbols. The number of the feedback taps is $N_{fb} = 5$. In the PLL embedded in the DFE, the proportional tracking constant K_{f_1} and the integral tracking constant K_{f_2} are both set as 0.0002. The RLS forgetting factor λ in the DFE is chosen as 0.999.

As shown in Fig. 4(b), the output SNR at the two carrier frequencies exhibits significant change during the 12 h period of Event 50. For both carrier frequencies, the output SNR decreases during the period from 22:00 to 00:30 when the internal waves significantly overlap the acoustic track. As shown in Fig. 4(a), this period shows strong water column temperature fluctuations in the upper water column (about 20 m below the sea surface). The clear correlation between the water column characteristics and the communication performance strongly suggests that the internal waves degraded receiver performance because the water column was perturbed.

Furthermore, the internal wave effects are different at these two carrier frequencies. At $f_c = 813$ Hz, the performance degradation caused by the internal waves is relatively larger: The maximal difference in the output

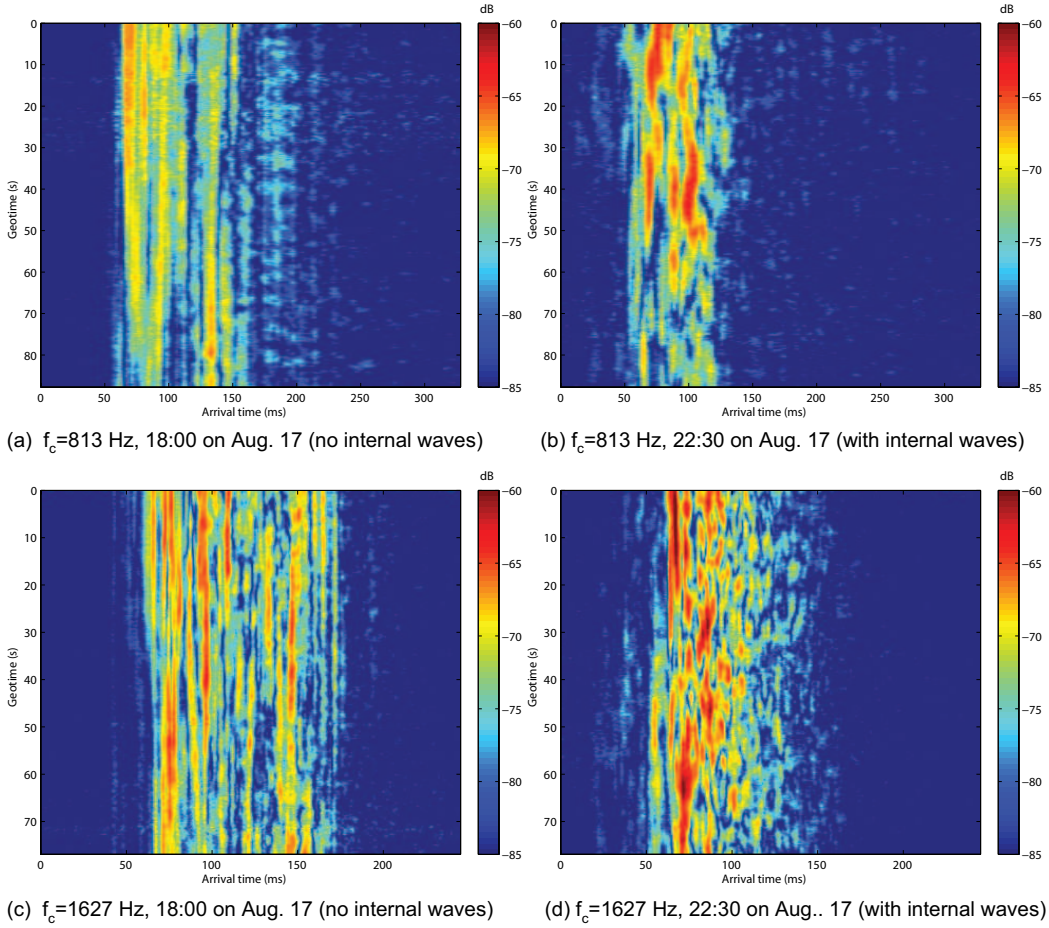

Figure 3: Estimated CIR functions at $f_c = 813$ Hz are shown (a) at 18:00 and (b) at 22:30 on Aug. 17, 2006. Estimated CIR functions at $f_c = 1627$ Hz are shown (c) at 18:00 and (d) at 22:30 on Aug. 17, 2006. The CIR functions are obtained for 77.25 m depth on the WHOI-VLA.

SNR can be about 7 dB between the condition when this internal wave packet did not reach the acoustic track and the condition when internal waves were intersecting the acoustic track. At $f_c = 1627$ Hz, the maximal difference in the output SNR is about 5 dB. The minimum output SNR appears at 00:00 (for $f_c = 813$) and 00:30 (for $f_c = 1627$) on Aug 18, 2006, when the entire acoustic track was affected by the passing internal waves. Generally, the communication performance at higher carrier frequencies is worse than that at lower carrier frequencies. However, double bandwidth was used at $f_c = 1627$ Hz for communications as compared to $f_c = 813$ Hz. As a consequence, the average output SNR at $f_c = 1627$ Hz is slightly higher than that at $f_c = 813$ Hz for the 12 h period.

5 Conclusions

In summary, the communication performance results at carrier frequencies of 813 Hz and 1627 Hz has been reported to have significant change when the internal waves passed through the acoustic track during the SW06 experiment. The effects of the internal waves also show a frequency dependency. In the future studies, acoustic propagation models will be used to explain the performance variation and its frequency dependency at these two carrier frequencies. The optimization of receiver parameters under different environmental conditions will be another focus in the future studies.

Acknowledgments

This research was supported by the Office of Naval Research (ONR), Code 321OA. The authors wish to thank all participants of the SW06 experiment, especially the science crew aboard the R/V Sharp: Lauren Brown, Steve Crocker, Georges Dossot, Boris G. Katsnelson, Jeremie Largeaud, Jing Luo, Jakob Siegel, Lin Wan, and Jie Yang. We also thank the R/V Sharp crew for their help during the experiment.

References

[1] J. R. Apel, M. Badiey, C.-S. Chiu, S. Finette, R. Headrick, J. Kemp, J. F. Lynch, A. Newhall, M. H. Orr, B. H. Pasewark, D. Tielbuerger, A. Turgut, K. von der Heydt, and S. Wolf, "An overview of the 1995 SWARM shallow-water internal wave acoustic scattering experiment," IEEE J. Oceanic Eng. **22**(3), 465–500 (1997).

[2] M. Badiey, B. G. Katsnelson, J. F. Lynch, S. Pereselkov, and W. L. Siegmann, "Measurement and modeling of three-dimensional sound intensity vari-

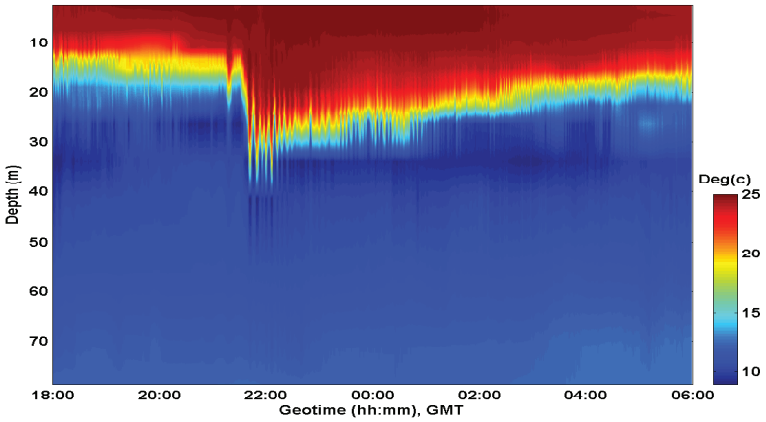

(a) Temperature profiles recorded at the WHOI-VLA

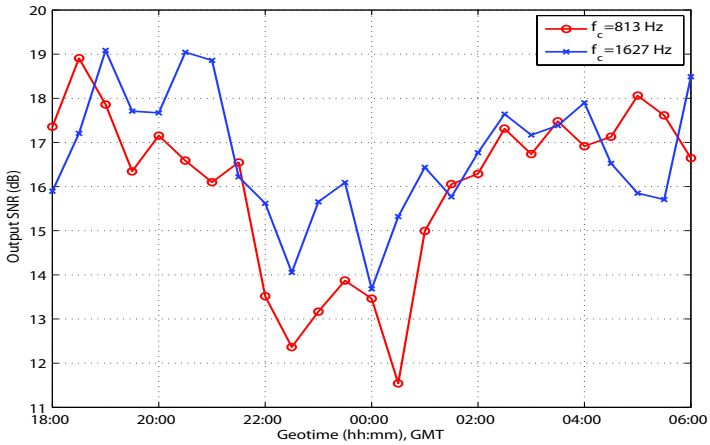

(b) The output SNR of the communication receiver

Figure 4: The temperature profiles and the receiver performance. (a) The temperature profiles recorded by the sensors attached to at the WHOI-VLA mooring (WHOI mooring # SW54). (b) The output SNR of the communication receiver for the BPSK signals at $f_c = 813$ Hz and $f_c = 1627$ Hz from 18:00 on Aug. 17 to 06:00 on Aug. 18, 2006 (Event 50).

ations due to shallow-water internal waves," J. Acoust. Soc. Am. **117**(2), 613–625 (2005).

[3] M. Badiey, B. G. Katsnelson, J. F. Lynch, and S. Pereselkov, "Frequency dependence and intensity fluctuations due to shallow water internal waves," J. Acoust. Soc. Am. **122**(2), 747–760 (2007).

[4] D. Rouseff, A. Turgut, S. N. Wolf, S. Finette, M. H. Orr, B. H. Pasewark, J. R. Apel, M. Badiey, C.-S. Chiu, R. H. Headrick, J. F. Lynch, J. N. Kemp, A. E. Newhall, K. von der Heydt, and D. Tielbuerger, "Coherence of acoustic modes propagating through shallow water internal waves," J. Acoust. Soc. Am. **111**(4), 1655–1666 (2002).

[5] T. C. Yang, "Environmental effects on phase coherent underwater acoustic communications: A perspective from several experimental measurements," in *High Freq. Ocean Acoust.* (AIP, New York, 2004), pp. 90–97.

[6] A. E. Newhall, T. F. Duda, J. D. I. K. von der Heydt, J. N. Kemp, S. A. Lerner, S. P. Liberatore, Y.-T. Lin, J. F. Lynch, A. R. Maffei, A. K. Morozov, A. Shmelev, C. J. Sellers, and W. E. Witzell, "Acoustic and oceanographic observations and configuration information for the WHOI moorings for the SW06 experiment," WHOI technical report #WHOI-2007-04, (2007).

[7] A. Song, M. Badiey, H.-C. Song, W. S. Hodgkiss, M. Porter, and the KauaiEx Group, "Impact of ocean variability on coherent underwater acoustic communications during the Kauai experiment (KauaiEx)," J. Acoust. Soc. Am. **123**(2), 856–865 (2008).

[8] G. F. Edelmann, H. C. Song, S. Kim, W. S. Hodgkiss, W. A. Kuperman, and T. Akal, "Underwater acoustic communications using time reversal," IEEE J. Oceanic Eng. **30**(4), 852–864 (2005).

[9] T. C. Yang, "Correlation-based decision-feedback equalizer for underwater acoustic communications," IEEE J. Oceanic Eng. **30**(4), 865–880 (2005).

[10] J. A. Flynn, J. A. Ritcey, D. Rouseff, and W. L. J. Fox, "Multichannel equalization by decision-directed passive phase conjugation: Experimental results," IEEE J. Oceanic Eng. **29**(3), 824–836 (2004).

[11] M. Stojanovic, J. A. Catipovic, and J. G. Proakis, "Phase-coherent digital communications for underwater acoustic channels," IEEE J. Oceanic Eng. **19**(1), 100–111 (1994).